⌘ *Author's Choice*

THE JOURNAL OF BIOLOGICAL CHEMISTRY VOL. 291, NO. 8, pp. 4178–4184, February 19, 2016

Purification of Active Respiratory Supercomplex from Bovine Heart Mitochondria Enables Functional Studies*

Received for publication, July 21, 2015, and in revised form, December 18, 2015 Published, JBC Papers in Press, December 23, 2015, DOI 10.1074/jbc.M115.680553

Kyoko Shinzawa-Itoh[‡1], Harunobu Shimomura[‡], Sachiko Yanagisawa[‡2], Satoru Shimada[‡§], Ryoko Takahashi[‡], Marika Oosaki[‡], Takashi Ogura[‡2], and Tomitake Tsukihara[‡§¶]

From the [‡]Department of Life Science, Graduate School of Life Science, University of Hyogo, 3-2-1, Koto, Kamighori, Akoh, Hyogo, 678-1297, Japan, [§]Core Research for Evolutional Science and Technology (CREST), Japan Science and Technology Agency, Kawaguchi, Saitama 332-0012, Japan, and [¶]Institute for Protein Research, Osaka University, 3-2 Yamadaoka, Suita, Osaka 565-0871, Japan

To understand the roles of mitochondrial respiratory chain supercomplexes, methods for consistently separating and preparing supercomplexes must be established. To this end, we solubilized supercomplexes from bovine heart mitochondria with digitonin and then replaced digitonin with amphipol (A8–35), an amphiphilic polymer. Afterward, supercomplexes were separated from other complexes by sucrose density gradient centrifugation. Twenty-six grams of bovine myocardium yielded 3.2 mg of amphipol-stabilized supercomplex. The purified supercomplexes were analyzed based on their absorption spectra as well as Q_{10} (ubiquinone with ten isoprene units) and lipid assays. The supercomplex sample did not contain cytochrome *c* but did contain complexes I, III, and IV at a ratio of 1:2:1, 6 molecules of Q_{10}, and 623 atoms of phosphorus. When cytochrome *c* was added, the supercomplex exhibited KCN-sensitive NADH oxidation; thus, the purified supercomplex was active. Reduced complex IV absorbs at 444 nm, so we measured the resonance Raman spectrum of the reduced amphipol-solubilized supercomplex and the mixture of amphipol-solubilized complexes I_1, III_2, and IV_1 using an excitation wavelength of 441.6 nm, allowing measurement precision comparable with that obtained for complex IV alone. Use of the purified active sample provides insights into the effects of supercomplex formation.

Oxidative phosphorylation in mitochondria is carried out by five large multisubunit complexes: complex I[3] (NADH dehydrogenase), complex II (succinate dehydrogenase), complex III (cytochrome *c* reductase/cytochrome bc_1 complex), complex IV (cytochrome *c* oxidase), and complex V (mitochondrial F_1F_o ATP synthase).

Complexes I, III, and IV catalyze the transfer of electrons from NADH to molecular oxygen and use the energy released by electron transfer to pump protons across the inner membrane. The mechanisms of electron transfer and proton pump reactions have been studied in individual respiratory complexes (1–11). However, little is known about how these complexes interact in the membrane to perform their tasks.

Two alternative models have been proposed for the arrangement of the respiratory chain complexes in the membrane. According to the random collision model (12), all components of the respiratory chain diffuse individually in the membrane, and electron transfer depends on random, transient encounters between individual protein complexes and smaller electron carriers. In the solid-state model (13) the substrate is channeled directly from one enzyme to the next within supercomplexes, which reflects a higher level of organization.

The solid-state model gained support from the discovery of supercomplexes in bovine heart and yeast mitochondria by blue native polyacrylamide gel electrophoresis (BN-PAGE) (14). The exact reasons for their presence remain elusive. It is possible that the supercomplex formation could enhance the electron flow between these complexes, stabilize individual complexes, and prevent the formation of oxygen radicals (15–23).

Single-particle electron cryomicroscopy and cryoelectron tomography has enabled three-dimensional reconstruction of supercomplexes at 19 Å, 22 Å, and 24 Å resolution using small purified samples from bovine heart (24, 25) and *Saccharomyces cerevisiae* (26). These structures have provided insight into the interactions between these complexes.

Here we report the purification from bovine heart (26 g) of amphipol-solubilized supercomplex (3.2 mg) consisting of complex I_1, complex III_2, complex IV_1, and six molecules of Q_{10} (suffixes on Roman numerals indicate the number of oligomers in each complex). The purified supercomplexes exhibited KCN-sensitive NADH oxidation activities upon the addition of cytochrome *c*. Absorption spectrum and resonance Raman spectrum measurement of purified samples enabled functional investigations of the supercomplex.

Experimental Procedures

Preparation of Supercomplex—Bovine heart mitochondria were prepared by differential centrifugation as described in Smith (27). Mitochondria were solubilized with 6% (w/v) digitonin (Calbiochem, high purity) in 1 M sucrose, 20 mM Tris-HCl (pH 8.0) at a detergent-to-protein weight ratio of 10:1. The samples was centrifuged at 65,000 × *g* for 5 min, and the

* This work was supported by CREST/JST and Grant-in-aid for Scientific Research on Innovative Areas (2503) 26104532, MEXT, Japan (to T. O.).

[1] To whom correspondence should be addressed. Tel.: 81-791-58-0191; E-mail: shinzawa@sci.u-hyogo.ac.jp.
[2] Both authors are visiting scientists at RIKEN.
[3] The abbreviations used are: complex I, NADH dehydrogenase; complex II, succinate dehydrogenase; complex III, cytochrome *c* reductase/cytochrome bc_1 complex; complex IV, cytochrome *c* oxidase; complex V, mitochondrial F_1F_o ATP synthase; complex I_1, complex III_2, complex IV_1, and complex V_1 suffixes of Roman numerals indicate the number of oligomers in each complex; Q_{10}, ubiquinone with 10 isoprene units; Q_1, ubiquinone with one isoprene unit; BN-PAGE, blue native-PAGE.

resultant supernatant was treated with amphipol (A8–35) (amphipol-to-protein ratio, 3:1) at 0 °C for 30 min. γ-Cyclodextrin (in the same detergent-to-protein ratio as digitonin) was added to the mixture, which was then incubated for 60 min at 4 °C. Precipitated material was removed by centrifugation at 65,000 × *g* for 10 min at 4 °C. The resultant supernatant was centrifuged on a stepwise sucrose gradient (1.6, 1.55, 1.5, 1.4, and 1.3 M sucrose in HEPES-Na (pH 7.8)) at 105,000 × *g* for 24 h at 4 °C. Gradients were fractionated from bottom to top, and protein content was investigated by BN-PAGE in linear gradient gels containing 3–10% polyacrylamide (Invitrogen). Protein concentration was determined by the Markwell procedure (28).

Sample Preparation for Spectroscopic Measurement—Protein (3.5–3.8 μM) was dissolved in HEPES-Na buffer (pH 7.8) with sucrose (0.1–1.3 M). The purified sample in oxidized form was transferred into a cylindrical quartz spinning Raman cell with a diameter of 3 mm. To reduce the protein, 10 mM of sodium dithionite was added, and the solution was agitated under anaerobic conditions.

Absorption Spectral Measurement—Absorption spectra from 700 to 350 nm were measured at room temperature using a spectrophotometer (U3310, HITACHI) with an attachment for the cylindrical Raman spinning cell. The sample concentration and composition were determined as follows: complex IV concentration was determined for the reduced form using an extinction coefficient of $\epsilon_{604-630} = 46.6\ mM^{-1}\ cm^{-1}$ (29). Concentrations of *c*-type cytochrome and *b*-type cytochrome were determined on redox difference spectra using $\epsilon_{553-544} = 19\ mM^{-1}\ cm^{-1}$ and $\epsilon_{562-577} = 20\ mM^{-1}\ cm^{-1}$, respectively (30).

Resonance Raman Measurement—A 5-milliwatt He-Cd laser (IK4101R-F, Kimmon Koha) was used for Raman measurement. The laser was focused on the sample in the spinning cell (1500 rpm) from below, and Raman scattering at 90° was directed to a Raman spectrometer (Chromex, 500IS); data were collected using a liquid N_2-cooled CCD detector (Roper Scientific, Spec-10:400B/LN). Indene and carbon tetrachloride were used as standards for frequency calibration. The resonance Raman spectra of supercomplex, mixtures of enzyme complexes, individual enzyme complexes, and sucrose solution were measured. For each sample 20 continuous 1-min measurements were carried out. After confirmation that there was no spectral change during 20 min of laser irradiation; all 20 spectra were combined into one spectrum. The contribution of sucrose to the Raman spectrum was subtracted with a reasonable coefficient. The absorption spectrum of each sample was monitored before and after Raman measurement to confirm the redox state of the sample.

Measurement of Ubiquinol (Q_{10}) and Phospholipids—Q_{10} was extracted from 0.4 nmol of purified supercomplex samples by adding isopropyl alcohol in the presence of Q_9 (ubiquinone with nine isoprene units) as an internal standard. Measurement of ubiquinol using LC/MS/MS (AB SCIEX QTRAP5500) was outsourced to Kaneka Techno Research. Phosphorus content of the sample solution was analyzed directly without extraction with an organic solvent, as described in Bartlett (31) and Shinzawa-Itoh *et al.* (32) with some modifications; 0.25 ml of 60% perchloric acid solution was added to 0.1 ml of sample solution containing various amounts (20–60 μg) of the protein, and the mixture was incubated overnight at 155 °C until a colorless transparent solution was obtained. After the solution was cooled to room temperature, 1.2 ml of 0.22% ammonium molybdate and 0.05 ml of 1% amidol dissolved in 20% sodium bisulfate were added, and the mixture was heated at 100 °C for 12 min. A glass ball was placed on the open end of the test tube to enable effective condensation of water vapor during the two heat treatments. Afterward, absorbance at 830 nm was determined. The phosphorus content was quantified by comparing the slope of the plot of the absorbance at 830 nm against the amount of protein with the slope of the standard sample (K_2HPO_4).

Enzyme Activity Assay—The reaction mixture (2.1–2.15 ml) contained 150 μM NADH in 100 mM potassium phosphate buffer (pH 8.0) at 20 °C in a quartz cuvette with a 1-cm light path. The cuvette was equipped with a magnetic stirrer and placed in a cuvette holder whose temperature was held constant by a circulating water system. The enzyme reaction was initiated by the addition of 10–20 μl of enzyme solution and 10 μl of 200 μM cytochrome *c* (horse heart) and followed by monitoring the decrease in absorbance at 340 nm. KCN inhibition was determined at a concentration of 2 mM inhibitor. After the addition of 4 μl of 20 mM Q_1, piericidin A inhibition was determined at a concentration of 10 μM.

Preparation of Amphipol-solubilized Complex I_1, Complex III_2, and Complex IV_1—Complex I was purified from bovine heart mitochondria as described previously (32, 33), except that the ammonium fractionation was omitted. The enzyme fraction, purified by anion-exchange column chromatography, was treated with amphipol (amphipol-to-protein weight ratio, 3:1). Two milliliters of 1% (W/V) β-cyclodextrin was added to the mixture and dialyzed for 60 min at 4 °C against 100 ml of 40 mM HEPES-Na (pH 7.8) containing 1% (W/V) β-cyclodextrin. The resultant mixture was centrifuged on a stepwise sucrose gradient (1.15, 1.1, 1.05, 1.1, and 0.9 M sucrose in HEPES-Na (pH 7.8)) at 105,000 × *g* for 3 h at 4 °C. Gradients were fractionated from bottom to top, and protein content was investigated by BN-PAGE in linear gradient gels containing 3–12% polyacrylamide. The enzyme activity of the amphipol-solubilized preparation, which was monitored by following NADH-Q_1 oxidoreduction at 20 °C, was 1.5–2.1 μmol/min/nmol. This activity was 95.0–99.7% inhibited by piericidin A.

Complex III crystalline sample (24.8 mg) solubilized with 0.2% (w/v) 6-cyclohexyl-1-hexyl-maltopyranoside in 40 mM Tris-Cl buffer (pH 8.0) (34) was treated with amphipol (amphipol-to-protein weight ratio, 3:1). Two milliliters of 1% (w/v) β-cyclodextrin was added to the mixture, which was then dialyzed against 100 ml of 40 mM HEPES-Na (pH 7.8) containing 1% (w/v) β-cyclodextrin for 60 min at 4 °C. The resultant mixture was centrifuged on a stepwise sucrose gradient (1.2, 1.1, 1.0, 0.9, and 0.8 M sucrose in HEPES-Na (pH 7.8)) at 105,000 × *g* for 15 h at 4 °C. Gradients were fractionated from bottom to top, and protein content was investigated by BN-PAGE. The resultant amphipol-solubilized complex III existed as a dimer, complex III_2, and the ratio of cytochrome *b*/cytochrome c_1 was 1.95.

Crystalline complex IV (5 mg) solubilized with 0.2% (w/v) *n*-decyl-β-D-maltoside in 100 mM sodium phosphate buffer

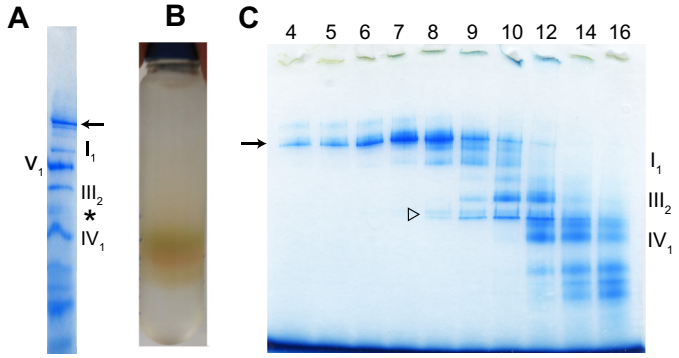

FIGURE 1. **Purification of supercomplex.** *A*, BN-PAGE pattern of bovine heart mitochondria after membrane proteins were solubilized with digitonin. *Arrow*: supercomplex. The faint broad band (*) contained a complex IV dimer. *B*, separation of supercomplex and respiratory complexes by centrifugation on a stepwise sucrose gradient. After centrifugation at 105,000 × *g* for 24 h, bands of several different colors were produced. *C*, gradients were fractionated from *bottom to top*, and protein content was investigated by BN-PAGE in linear gradient gels containing 3–12% polyacrylamide. *White arrow head*: degraded complex V during the process of sucrose density gradient centrifugation.

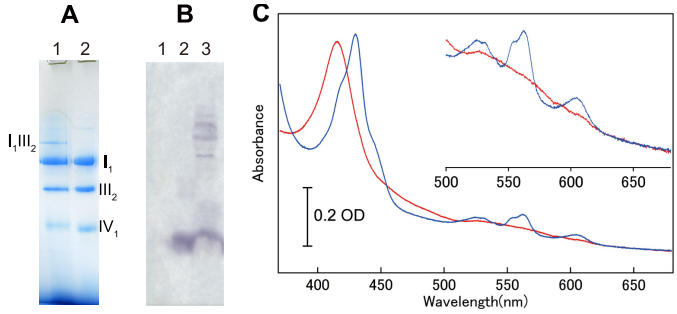

FIGURE 2. **Characterization of the purified supercomplex.** *A*, BN-PAGE pattern of treated amphipol-solubilized supercomplex (*lane 1*) and mixture of purified complexes I_1, III_2, and IV_1 (*lane 2*). 11 μg of amphipol-solubilized supercomplex was treated with 40 mM HEPES-Na (pH 7.8) containing 50 mM KCl and 0.25% (W/V) lauryl maltose neopentyl glycol. The mixture contained 5.0 μg of complexes I_1, 2.5 μg of complex III_2 and 1.0 μg of complex IV_1. *B*, Western blotting pattern using anti-cytochrome *c* antibody. 94 μg of supercomplex (*lane 1*), 1.0 μg of horse heart cytochrome *c*, and 120 μg of SDS-solubilized mitochondria membrane (*lane 3*) were loaded and transferred to PVDF membrane. *C*, the absorption spectra of both the oxidized complex as isolated (*red*) and the dithionite-reduced complex (*blue*).

(pH 7.4) (29) was treated with 2% (w/v) *n*-octyl-β-D-glucoside at 0 °C for 120 min before the addition of amphipol (amphipol-to-protein weight ratio, 3:1). One milliliter of 1% (w/v) β-cyclodextrin was added to the mixture, which was then dialyzed against 100 ml of 40 mM HEPES-Na (pH 7.8) containing 1% (w/v) β-cyclodextrin for 60 min at 4 °C. The resultant mixture was centrifuged on a stepwise sucrose gradient (1.350, 1.338, 1.325, 1.315, 1.3, and 1.2 M sucrose in HEPES-Na (pH 7.8)) at 105,000 × *g* for 24 h at 4 °C. Gradients were fractionated from bottom to top, and protein content was investigated by BN-PAGE.

Immunoblotting—After electrophoresis the complexes were electroblotted onto PVDF membranes and sequentially probed with specific monoclonal antibodies against anti-cytochrome *c* (Invitrogen). Final detection was performed with secondary antibodies linked to horseradish peroxidase (GE Healthcare) using 4-chloro-1-naphthol.

Results and Discussion

Preparation of an Amphipol-solubilized Supercomplex from Bovine Heart Mitochondria—Fractions of bovine heart mitochondria were solubilized with digitonin and separated using BN-PAGE. This resulted in detection of a band (Fig. 1*A*) that was presumed to be a supercomplex. The supercomplex was larger than complex I, with a mass of 1000 kDa. In addition to the supercomplex and complex I, complex V_1, complex III_2, and complex IV monomer were also visible. The faint broad band (*) contained a complex IV dimer that was present at a markedly lower level than complex IV monomer.

Amphipol (at a weight ratio of 3:1 relative to mitochondrial protein) was added to the digitonin-solubilized fractions, γ-cyclodextrin was used to remove digitonin, and the fractions were subjected to sucrose density gradient centrifugation. After centrifugation at 105,000 × *g* for 24 h, bands of several different colors were produced, and separation of the complexes was apparent (Fig. 1*B*). Aliquots (200 μl) were taken from the bottom of the centrifuge tube, and the proteins contained in each fraction were identified by BN-PAGE (Fig. 1*C*). Protein complexes were separated by sucrose density gradient centrifugation; the bands with the darkest colors, closest to the bottom of the centrifuge tube, were determined to contain supercomplexes.

Complex V was degraded during the process of sucrose density gradient centrifugation, and bands between complex III_2 and complex IV_1 (about 400 kDa: *white arrow head* in Fig. 1*C*) were visible. Fractions 4–7 contained almost exclusively supercomplex. Supercomplexes solubilized by amphipol were successfully separated and purified. With a high level of reproducibility, 26 g of bovine myocardium yielded a mitochondrial fraction of 72 mg, which in turn yielded about 3.2 mg of supercomplex. Yield could be significantly increased by promptly solubilizing the prepared mitochondrial membranes with digitonin.

Characterization of the Purified Supercomplex—BN-PAGE revealed a band (*arrow* in Fig. 1, *A* and *C*) that was presumed to represent a supercomplex larger than complex I with a mass of 1000 kDa. To demonstrate that this supercomplex band contained complexes I, III, and IV, amphipol-solubilized supercomplex was treated with 40 mM HEPES-Na (pH 7.8) containing 50 mM KCl and 0.25% (w/v) lauryl maltose neopentyl glycol overnight at 4 °C. After this treatment bands derived from complexes I_1, III_2, and IV_1 were observed in BN-PAGE (Fig. 2*A*). The supercomplex was dissociated into complexes I_1, III_2, and IV_1. The faint band, larger than complex I, contained a complex of I_1 and III_2; complex IV was removed from supercomplex. The presence of complex III and IV was also clearly demonstrated by the absorption spectra, whereas complex I could not be detected. However, complex I was clearly detected in BN-PAGE pattern. Together, these results show that the supercomplex consisted of complexes I, III, and IV.

Absorption spectra for the oxidized and sodium dithionate-reduced forms of amphipol-solubilized supercomplex are shown in Fig. 2*C*. The absorption spectra of the reduced form exhibited peaks at 553, 562, and 604 nm due to the presence of *c*-type, *b*-type, and *a*-type cytochrome, respectively. For this study we prepared several samples of supercomplex, with the

TABLE 1
Concentration of cytochromes in each supercomplex samples

Sample	*b*-Type	*c*-Type	*b*-Type/*c*-Type	IV_1	*b*-Type/IV_1	*c*-Type/IV_1
	μM	μM		μM		
1	9.46	5.15	1.84	2.23	4.24	2.31
2	5.09	2.83	1.80	1.18	4.32	2.40
3	9.16	5.08	1.80	2.68	3.41	1.90
4	9.25	4.80	1.93	2.13	4.34	2.25
5	8.20	4.67	1.76	2.14	3.83	2.18
6	8.60	5.00	1.72	2.40	3.58	2.08
7	13.70	8.57	1.60	3.89	3.52	2.20
8	13.50	7.93	1.70	3.53	3.82	2.25
Average (S.D.)			1.77 (0.09)		3.88 (0.35)	2.20 (0.14)

concentration of complex IV_1 ranging from 2.0 to 3.8 μM. We measured the absorption spectra of these samples and determined the concentrations of the cytochromes in each. The ratio of *b*-type to *c*-type cytochrome was close to 2 (1.77 ± 0.092; $n = 8$). The ratio of *b*-type cytochrome to complex IV monomer was 3.88 ± 0.35 ($n = 8$), and the ratio of *c*-type cytochrome to complex IV monomer was 2.20 ± 0.14 ($n = 8$). These findings revealed that the samples did not contain cytochrome *c* (Table 1), which was confirmed immunochemically (Fig. 2*B*). Previous research revealed a structure with one molecule of cytochrome *c* bound to the complex III dimer, and that study suggested that cytochrome *c* was present in the supercomplex (24). However, the measurements reported here strongly indicate that cytochrome *c* was not present in our supercomplex sample, possibly because the binding of cytochrome *c* and complex III was not strong enough to withstand the process of sucrose density gradient centrifugation. Complex I has a mass of 1,000 kDa, and its mobility in BN-PAGE indicated that it is unlikely to form a dimer. Thus, the prepared supercomplex consisted of complex I, complex III, and complex IV at a ratio of 1:2:1 but did not contain cytochrome *c*.

We then determined the amount of Q_{10} per complex IV_1, *i.e.* the amount of Q_{10} contained in one molecule of the supercomplex. The results of this analysis revealed that the supercomplex contained 6.23 ± 1.11 ($n = 6$) molecules of Q_{10}. This Q_{10} was detected only in the oxidized form but not in the reduced form. Similarly, we determined the amount of Q_{10} in the mitochondrial membrane and found that there were 6.30 ± 0.37 ($n = 7$) molecules of Q_{10} per complex IV_1. There was no difference between the contents of Q_{10} per complex IV_1 in supercomplex and mitochondrial membrane. These results indicate that there was no specific uptake of Q_{10} by the supercomplex and support the idea that Q exists as a common pool in mitochondria that is exchanged freely between complexes (35). The purified sample of complex I_1 contained one molecule of Q_{10} (32). The crystalline sample of complex III_2 prepared by our method (34) contained 1.00 ± 0.08 ($n = 4$) molecules of Q_{10} per complex III dimer. Presumably, these Q_{10} molecules bind strongly to enzymes and play a role in the function of each complex. The supercomplex purified in this study contained six molecules of Q_{10}; four of these molecules facilitate electron transfer between complexes I and III, as is discussed later.

In the supercomplex individual complexes are thought to assemble via lipids, and the association of individual complexes strongly depends on the amount and composition of lipids (26, 36, 37). To estimate the phospholipid content in the supercomplex, we assayed phosphorus. The results revealed that each mol of supercomplex contained 623 ± 102 mol ($n = 7$) phosphorus. Purified complex I_1 and the crystalline samples of complex III_2 and complex IV_1 contained 71, 108, and 13 mol of phosphorus, respectively (32, 34, 36). These phospholipids found in complexes I_1, III_2, and IV_1 are specifically bound to the protein moiety; in other words, all of these phospholipids are intrinsic constituents of these complexes. The cryo-EM maps of the yeast and bovine supercomplexes showed that complexes I_1, III_2, and IV_1 are some distance apart within the supercomplexes (24–26). In our supercomplex samples, each mol of supercomplex contained 623 mol of phosphorus, greater than the total phosphorus contents of individual complexes. The space between the individual complexes is most likely to be filled with these lipids.

Next we examined the composition of phospholipids in the supercomplex. To this end we extracted lipids from the supercomplex and qualitatively analyzed them by mass spectroscopy. As described in a previous report (36), we analyzed the lipids of each purified respiratory complex (I, III, IV, and V). This analysis revealed the presence of cardiolipin (C = 18:2), phosphatidylethanolamine (C = 18:0,20:4), phosphatidylcholine (C = 16:0,18:2) (C = 16:0,18:1), choline plasmalogen (C = 16:0,18:2) (C = 16:0,18:1), and phosphatidylglycerol (C = 16:0,18:1). These respiratory complexes contain these seven species of phospholipids in varying ratios. The types of lipids that the supercomplex contained coincided with the lipids contained in individual complexes, as previous studies have reported (36).

Several studies have reported that cardiolipin is essential for the formation of supercomplexes (37, 38). Therefore, we examined the cardiolipin and phosphatidylethanolamine content in the supercomplex: 50–90 mol of cardiolipin and 180–250 mol of phosphatidylethanolamine were present per mol of supercomplex (determined in three independent experiments). The proportions of phosphorus in these lipids relative to total phosphorus in supercomplex samples differed little from their proportions in the mitochondrial membrane; thus, it is unlikely that cardiolipin and phosphatidylethanolamine are specifically involved in these interactions. It is not clear how cardiolipin can play an important role in the interaction between individual complexes but not specifically in supercomplex formation.

Activity of the Purified Supercomplex—Next, we measured the oxidation of NADH by supercomplexes at 20 °C and compared the electron transfer reactions with those of a mixture of purified complexes I_1, III_2, and IV_1.

Complex IV in the supercomplex exists as a monomer. Because the enzyme purified with *n*-decyl-β-D-maltoside is

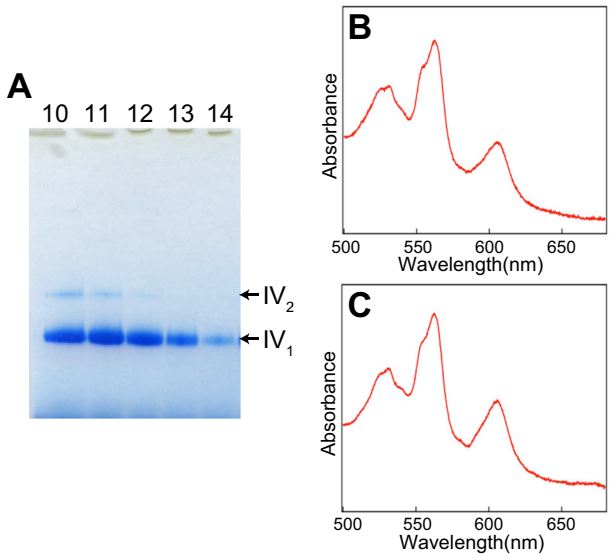

FIGURE 3. **Preparation of amphipol-solubilized mixture of complexes I_1, III_2, and IV_1.** *A*, preparation of complex IV monomer. After centrifugation on a stepwise sucrose gradient, gradients were fractionated from *bottom to top*, protein content was investigated by BN-PAGE on linear gradient gels containing 3–12% polyacrylamide. Fractions 13 and 14 were collected as complex IV_1. *B*, absorption spectra of the dithionite-reduced supercomplex. *C*, absorption spectra of dithionite-reduced mixture of complexes I_1, III_2, and IV_1.

present as a balance of monomer and dimer, we prepared monomer complex IV from *n*-decyl-β-D-maltoside-solubilized enzyme by replacing the detergent with amphipol and separating the sample by sucrose density gradient centrifugation, as confirmed by BN-PAGE (Fig. 3*A*). On the other hand, the mixture of each individual component of the supercomplex requires complex I_1 and complex III_2 in addition to the complex IV monomer. Previously, we successfully generated two- or three-dimensional crystals of complex I, complex III, and complex IV (10, 33, 34). From these highly pure samples, complex I_1 and complex III_2 as well as complex IV_1 were prepared with amphipol in the same manner as in the supercomplex preparation. These enzyme complexes exhibited absorption spectra very similar to those of enzyme complexes solubilized with a surfactant. The mixture of amphipol-solubilized complex I_1, III_2, and IV_1 exhibited a spectrum almost identical with that of the amphipol-solubilized supercomplex (Fig. 3, *B* and *C*).

In the case of the supercomplex, oxidation of NADH was not detected even when enzyme was added to 100 mM potassium phosphate buffer (pH 7.8) containing 150 μM NADH. However, when oxidized cytochrome *c* was added at a final concentration of 1.0 μM, oxidation of NADH was observed. The addition of 2 mM KCN, a complex IV inhibitor, inhibited supercomplex activity, and added cytochrome *c* was completely reduced. After the addition of 50 μM Q_1, oxidation of NADH re-started. The addition of 10 μM piericidin A, an inhibitor of complex I, inhibited NADH oxidation by complex I in the supercomplex (Fig. 4*A*). In the case of the mixture of purified complex I_1, III_2, and IV_1, oxidation of NADH was not observed after the addition of 1.0 μM oxidized cytochrome *c*. After the addition of Q_1, oxidation of NADH started. The addition of piericidin A inhibited NADH oxidation by complex I (Fig. 4*B*). These findings

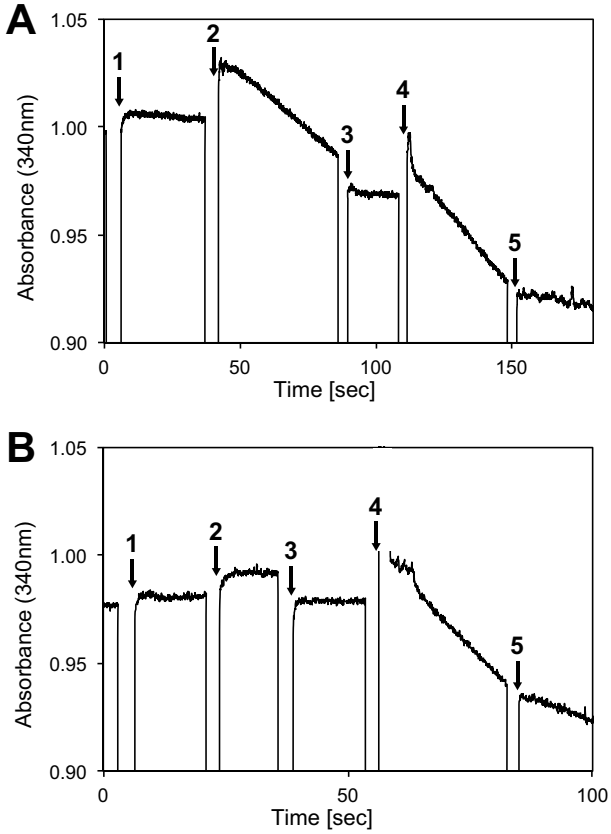

FIGURE 4. **Activity measurements of the electron transfer reaction from NADH to O_2 of purified supercomplex (*A*) and the mixture of purified complexes I_1, III_2, and IV_1 (*B*).** The reaction mixture contained 150 μM NADH in 100 mM potassium phosphate buffer (pH 8.0) at 20 °C. The enzyme reaction was initiated by the addition of 10–20 μl of the enzyme solution (*1*) and 10 μl of 200 μM cytochrome *c* (*2*) and followed by monitoring the decrease in absorbance at 340 nm. KCN inhibition (*3*) was determined at a concentration of 2 mM inhibitor. After the addition of 4 μl of 25 mM Q_1 (*4*), piericidin A inhibition (*5*) was determined at a concentration of 10 μM.

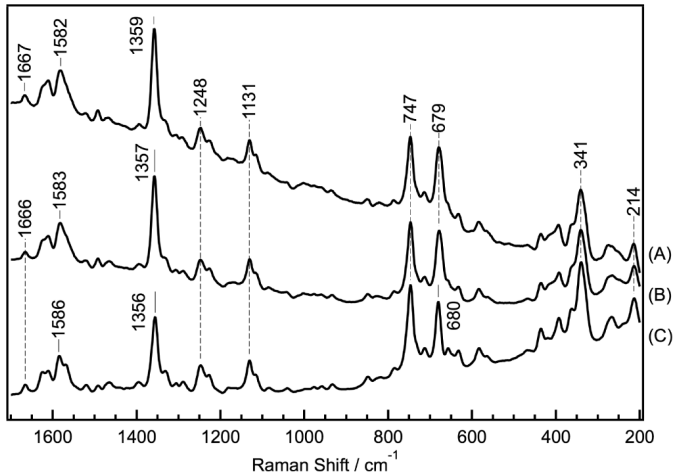

FIGURE 5. **Resonance Raman spectra of fully reduced amphipol-solubilized samples.** Supercomplex (*A*), mixture of amphipol-solubilized complex I_1, complex III_2, and complex IV_1 (*B*), and amphipol-solubilized complex IV monomer (*C*).

indicate that electron transfer from NADH to O_2 by the six molecules of Q_{10} contained in the supercomplex and the added cytochrome *c* was facilitated by complex I_1, complex III_2, and complex IV_1 contained within the supercomplex. The NADH oxidation rate of the supercomplex after the addition of cyto-

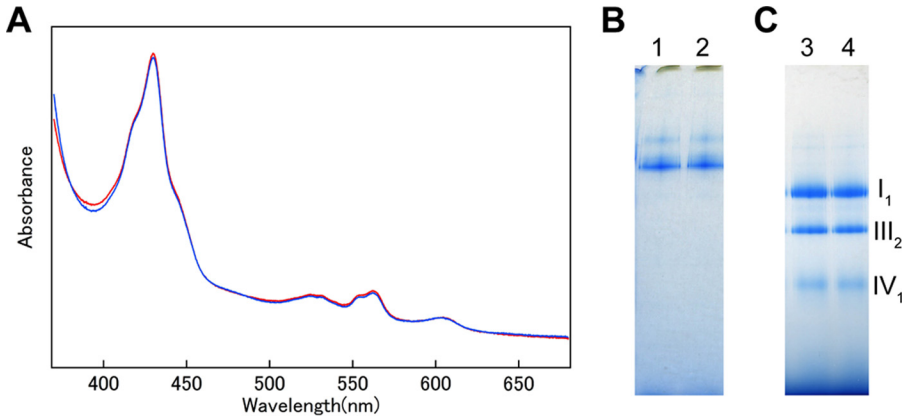

FIGURE 6. **Absorption spectra and BN-PAGE pattern before and after measurements of Resonance Raman spectra.** *A*, absorption spectra of fully reduced amphipol-solubilized supercomplex before (*red*) and after (*blue*) measurements of Resonance Raman spectra. *B*, BN-PAGE pattern of the supercomplex and *C*, mixture of complexes I_1, III_2, and IV_1. *Lanes 1* and *3*, before measurement of Resonance Raman spectra. *Lanes 2* and *4*, after measurement of Resonance Raman spectra.

chrome *c* was 0.48–0.74 μmol/min/nmol supercomplex (determined in 4 independent preparations). Furthermore, the rate of electron transfer from NADH to Q_1 by complex I in supercomplex, after inhibition by KCN, was 0.70–1.12 μmol/min/nmol. The rate of electron transfer from NADH to Q_1 in mixtures of individual complexes was 0.68–1.11 μmol/min/nmol complex I in supercomplex (determined in three independent preparations). The measured level of activity was appropriate given that the six molecules of Q_{10} contained in each supercomplex transfer electrons between complexes I and III. Thus, the prepared supercomplex was active and retained this activity for at least 7 days on ice.

Raman Spectra of the Supercomplex and Mixture of Complex I_1, Complex III_2, and Complex IV_1—To determine whether the prepared supercomplex was suitable for Raman spectroscopy, with the goal of examining the effect of the intermolecular interaction of individual complexes in the supercomplex on the enzyme reaction center, we measured the resonance Raman spectra of the prepared supercomplex and mixture of prepared individual complexes. The largest body of Raman spectral data has been assembled for complex IV. Reduced heme *a* has an absorption maximum at 444 nm, so the reduced form of the supercomplex was excited using a 441.6-nm laser to measure its resonance Raman spectrum. Fig. 5 shows resonance Raman spectra of the supercomplex (A), the mixture of individual complex (B), and the monomer of complex IV (C). The resonance Raman spectrum of the monomer complex IV (Fig. 5*C*) shows the formyl $\nu_{CH=O}$ of heme a_3 at 1666 cm^{-1}, ν_2 at 1586 cm^{-1}, ν_4 at 1356 cm^{-1}, ν_{16} at 747 cm^{-1}, ν_7 at 680 cm^{-1}, ν_8 at 341 cm^{-1}, and $\nu_{Fe\text{-}His}$ at 214 cm^{-1}(39), indicating that complex IV was in the fully reduced form. Furthermore, the spectrum is identical to that of *n*-decyl-β-D-maltoside-solubilized complex IV. There was no change in the absorption spectra (Fig. 6*A*) or BN-PAGE pattern (Fig. 6, *B* and *C*) as a result of the Raman measurement, indicating that laser illumination did not induce any change in the supercomplex. The resonance Raman spectra of the supercomplex (Fig. 5*A*) and mixture of the individual complexes (Fig. 5*B*) were essentially identical to that of the monomer of complex IV (Fig. 5*C*) because the excitation wavelength was adjusted for reduced complex IV. Thus, the spectra obtained for the supercomplex and mixtures were presumed to be due to the presence of complex IV_1 in each solution. On the other hand, the resonance Raman spectrum of the supercomplex (Fig. 5*A*) was more similar to that of the mixture (Fig. 5*B*) than that of the monomer (Fig. 5*C*). This is reasonable because the mixture contains the same amount of enzyme complexes as the supercomplex, including *b*- and *c*-type hemes, as confirmed by their comparable absorption spectra (Fig. 3, *B* and *C*). The qualities of the Raman spectra among these three samples were equivalent, and even single vibrational modes, such as $\nu_{CH=O}$ of heme a_3 and $\nu_{Fe\text{-}His}$ of complex IV, were detectable in the Raman spectrum of the supercomplex, which had a mass of 1700 kDa. Thus, we can confidently say that our supercomplex and prepared individual complexes were suitable for Raman measurement. It should be possible to perform further studies to confirm the effect of supercomplex formation on each complex, *e.g.* on the dynamics of electron transfer or CO binding to the supercomplex, as a proof of O_2 binding.

Thus far, the pseudo-atomic resolution structure of the supercomplex has been described by combining electron microscopy (cryo-EM maps) at a resolution of 19 Å and the x-ray structures of its components (24). In the supercomplex structure, individual complexes are adjacent, but there is no direct interaction between the proteins. The steric structure of the supercomplex must be determined to establish whether protein interactions are mediated by lipids.

Author Contributions—T. T. and K. S.-I. designed the research; H. S., S. Y., S. S., R. T., M. O., T. O., T. T., and K. S.-I. performed the research; purification and biochemical studies were performed by H. S., S. S., R. T., M. O., and K. S.-I; spectroscopic measurement was performed by H. S., S. S., S. Y., and K. S.-I. S. Y., and T. T; K. S.-I. wrote the paper.

Acknowledgment—We thank Dr. Shinya Yoshikawa (University of Hyogo) for encouragement.

References

1. Sazanov, L. A., and Hinchliffe, P. (2006) Structure of the hydrophilic domain of respiratory complex I from *Thermus thermophilus*. *Science*

311, 1430–1436
2. Zickermann, V., Wirth, C., Nasiri, H., Siegmund, K., Schwalbe, H., Hunte, C., and Brandt, U. (2015) Mechanistic insight from the crystal structure of mitochondrial complex I. *Science* **347,** 44–49
3. Vinothkumar, K. R., Zhu, J., and Hirst, J. (2014) Architecture of mammalian respiratory complex I. *Nature* **515,** 80–84
4. Zhang, Z., Huang, L., Shulmeister, V. M., Chi, Y. I., Kim, K. K., Hung, L. W., Crofts, A. R., Berry, E. A., and Kim, S. H. (1998) Electron transfer by domain movement in cytochrome bc_1. *Nature* **392,** 677–684
5. Iwata, S., Lee, J. W., Okada, K., Lee, J. K., Iwata, M., Rasmussen, B., Link, T. A., Ramaswamy, S., and Jap, B. K. (1998) Complete structure of the 11-subunit bovine mitochondrial cytochrome bc_1 complex. *Science* **281,** 64–71
6. Huang, L. S., Cobessi, D., Tung, E. Y., and Berry, E. A. (2005) Binding of the respiratory chain inhibitor antimycin to the mitochondrial bc_1 complex: a new crystal structure reveals an altered intramolecular hydrogen-bonding pattern. *J. Mol. Biol.* **351,** 573–597
7. Lange, C., Nett, J. H., Trumpower, B. L., and Hunte, C. (2001) Specific roles of protein-phospholipid interactions in the yeast cytochrome bc_1 complex structure. *EMBO J.* **20,** 6591–6600
8. Solmaz, S. R., and Hunte, C. (2008) Structure of complex III with bound cytochrome *c* in reduced state and definition of a minimal core interface for electron transfer. *J. Biol. Chem.* **283,** 17542–17549
9. Iwata, S., Ostermeier, C., Ludwig, B., and Michel, H. (1995) Structures at 2.8 Å resolution of cytochrome *c* oxidase from *Paracoccus denitrificans*. *Nature* **376,** 660–669
10. Tsukihara, T., Aoyama, H., Yamashita, E., Tomizaki, T., Yamaguchi, H., Shinzawa-Itoh, K., Nakashima, R., Yaono, R., and Yoshikawa, S. (1995) Structures of metal sites of oxidized bovine heart cytochrome *c* oxidase at 2.8 Å. *Science* **269,** 1069–1074
11. Tsukihara, T., Aoyama, H., Yamashita, E., Tomizaki, T., Yamaguchi, H., Shinzawa-Itoh, K., Nakashima, R., Yaono, R., and Yoshikawa, S. (1996) The whole structures of the 13-subunit oxidized cytochrome *c* oxidase at 2.8 Å. *Science* **272,** 1136–1144
12. Hackenbrock, C. R., Chazotte, B., and Gupte, S. S. (1986) The random collision model and a critical assessment of diffusion and collision in mitochondrial electron transport. *J. Bioenerg. Biomembr.* **18,** 331–368
13. Chance, B., and Williams, G. R. (1955) Respiratory enzymes in oxidative phosphorylation. III. The steady state. *J. Biol. Chem.* **217,** 409–427
14. Schägger, H., and Pfeiffer, K. (2000) Supercomplexes in the respiratory chains of yeast and mammalian mitochondria. *EMBO J.* **19,** 1777–1783
15. Acín-Pérez, R., Bayona-Bafaluy, M. P., Fernández-Silva, P., Moreno-Loshuertos, R., Pérez-Martos, A., Bruno, C., Moraes, C. T., and Enríquez, J. A. (2004) Respiratory complex III is required to maintain complex I in mammalian mitochondria. *Mol. Cell* **13,** 805–815
16. Maranzana, E., Barbero, G., Falasca, A. I., Lenaz, G., and Genova, M. L. (2013) Mitochondrial respiratory supercomplex association limits production of reactive oxygen species from complex I. *Antioxid. Redox Signal.* **19,** 1469–1480
17. Genova, M. L., and Lenaz, G. (2014) Functional role of mitochondrial respiratory supercomplexes. *Biochim. Biophys. Acta* **1837,** 427–443
18. Diaz, F., Fukui, H., Garcia, S., and Moraes, C. T. (2006) Cytochrome *c* oxidase is required for the assembly/stability of respiratory complex I in mouse fibroblasts. *Mol. Cell Biol.* **26,** 4872–4881
19. Chen, Y. C., Taylor, E. B., Dephoure, N., Heo, J. M., Tonhato, A., Papandreou, I., Nath, N., Denko, N. C., Gygi, S. P., and Rutter, J. (2012) Identification of a protein mediating respiratory supercomplex stability. *Cell Metab.* **15,** 348–360
20. Chaban, Y., Boekema, E. J., and Dudkina, N. V. (2014) Structures of mitochondrial oxidative phosphorylation supercomplexes and mechanisms for their stabilization. *Biochim. Biophys. Acta* **1837,** 418–426
21. Acin-Perez, R., and Enriquez, J. A. (2014) The function of the respiratory supercomplexes: the plasticity model. *Biochim. Biophys. Acta* **1837,** 444–450
22. Lapuente-Brun, E., Moreno-Loshuertos, R., Acín-Pérez, R., Latorre-Pellicer, A., Colás, C., Balsa, E., Perales-Clemente, E., Quirós, P. M., Calvo, E., Rodríguez-Hernández, M. A., Navas, P., Cruz, R., Carracedo, Á., López-Otín, C., Pérez-Martos, A., Fernández-Silva, P., Fernández-Vizarra, E., and Enríquez, J. A. (2013) Supercomplex assembly determines electron flux in the mitochondrial electron transport chain. *Science* **340,** 1567–1570
23. Ikeda, K., Shiba, S., Horie-Inoue, K., Shimokata, K., and Inoue, S. (2013) A stabilizing factor for mitochondrial respiratory supercomplex assembly regulates energy metabolism in muscle. *Nat. Commun.* **4,** 2147
24. Althoff, T., Mills, D. J., Popot, J.-L., and Kühlbrandt, W. (2011) Arrangement of electron transport chain components in bovine mitochondrial supercomplex $I_1III_2IV_1$. *EMBO J.* **30,** 4652–4664
25. Dudkina, N. V., Kudryashev, M., Stahlberg, H., and Boekema, E. J. (2011) Interaction of complexes I, III, and IV within the bovine respirasome by single particle cryoelectron tomography. *Proc. Natl. Acad. Sci. U.S.A.* **108,** 15196–15200
26. Mileykovskaya, E., Penczek, P. A., Fang, J., Mallampalli, V. K., Sparagna, G. C., and Dowhan, W. (2012) Arrangement of the respiratory chain complexes in *Saccharomyces cerevisiae* supercomplex III_2IV_2 revealed by single particle cryo-electron microscopy. *J. Biol. Chem.* **287,** 23095–23103
27. Smith, A. L. (1967) Preparation, properties, and conditions for assay of mitochondria: slaughterhouse material, small-scale. *Methods Enzymol.* **10,** 81–86
28. Markwell, M. A., Haas, S. M., Tolbert, N. E., and Bieber, L. L. (1981) Protein determination in membrane and lipoprotein samples: manual and automated procedures. *Methods Enzymol.* **72,** 296–303
29. Mochizuki, M., Aoyama, H., Shinzawa-Itoh, K., Usui, T., Tsukihara, T., and Yoshikawa, S. (1999) Quantitative reevaluation of the redox active sites of crystalline bovine heart cytochrome *c* oxidase. *J. Biol. Chem.* **274,** 33403–33411
30. Hatefi, Y., Haavik, A. G., and Griffiths, D. E. (1962) Studies on the electron transfer system. XLI. Reduced coenzyme Q (QH_2)-cytochrome *c* reductase. *J. Biol. Chem.* **237,** 1681–1685
31. Bartlett, G. R. (1959) Phosphorus assay in column chromatography. *J. Biol. Chem.* **234,** 466–468
32. Shinzawa-Itoh, K., Seiyama, J., Terada, H., Nakatsubo, R., Naoki, K., Nakashima, Y., and Yoshikawa, S. (2010) Bovine heart NADH-ubiquinone oxidoreductase contains one molecule of ubiquinone with ten isoprene units as one of the cofactors. *Biochemistry* **49,** 487–492
33. Shimada, S., Shinzawa-Itoh, K., Amano, S., Akira, Y., Miyazawa, A., Tsukihara, T., Tani, K., Gerle, C., and Yoshikawa, S. (2014) Three-dimensional structure of bovine heart NADH:ubiquinone oxidoreductase (complex I) by electron microscopy of a single negatively stained two-dimensional crystal. *Microscopy* **63,** 167–174
34. Murakami, S., Shinzawa-Itoh, K., and Yoshikawa, S. (1998) Crystals of bovine heart ubiquinol-cytochrome *c* reductase diffracting x-rays up to 2.8 Å resolution at 276 K. *Acta Crystallogr. D Biol. Crystallogr.* **54,** 146–147
35. Blaza, J. N., Serreli, R., Jones, A. J., Mohammed, K., and Hirst, J. (2014) Kinetic evidence against partitioning of the ubiquinone pool and the catalytic relevance of respiratory-chain supercomplexes. *Proc. Natl. Acad. Sci. U.S.A.* **111,** 15735–15740
36. Shinzawa-Itoh, K., Aoyama, H., Muramoto, K., Terada, H., Kurauchi, T., Tadehara, Y., Yamasaki, A., Sugimura, T., Kurono, S., Tsujimoto, K., Mizushima, T., Yamashita, E., Tsukihara, T., and Yoshikawa, S. (2007) Structures and physiological roles of 13 integral lipids of bovine heart cytochrome *c* oxidase. *EMBO J.* **26,** 1713–1725
37. Pfeiffer, K., Gohil, V., Stuart, R. A., Hunte, C., Brandt, U., Greenberg, M. L., and Schägger, H. (2003) Cardiolipin stabilizes respiratory chain supercomplexes. *J. Biol. Chem.* **278,** 52873–52880
38. Zhang, M., Mileykovskaya, E., and Dowhan, W. (2005) Cardiolipin is essential for organization of complex III and IV into a supercomplex in intact yeast mitochondria. *J. Biol. Chem.* **280,** 29403–29408
39. Ogura, T., Yoshikawa, S., and Kitagawa, T. (1985) Resonance Raman study on photoreduction of cytochrome *c* oxidase: distinction of cytochromes *a* and a_3 in the intermediate oxidation states. *Biochemistry* **24,** 7746–7752